



## QSAR MODELLING AND DOCKING ANALYSIS OF SOME THIAZOLE ANALOGUES AS $\alpha$ -GLUCOSIDASE INHIBITORS

M. T. Ibrahim<sup>1\*</sup>, A. Uzairu<sup>1</sup>, G. A. Shallangwa<sup>1</sup> and S. Uba<sup>1</sup>

<sup>1</sup>Department of Chemistry Ahamadu Bello University, P.M.B. 1044, Zaria Nigeria.

\*Corresponding author. Ahamadu Bello University, Department of Chemistry, Zaria, Kaduna, Nigeria, Phone: +2348069651985

e-mail address1: [muhdtk1988@gmail.com](mailto:muhdtk1988@gmail.com) (M. T. Ibrahim).

### ARTICLE INFO

Article history:

Received 2018-12-20

Accepted 2019-06-27

Available online 2019-06-30

### keywords

QSAR

Molecular modelling

Molecular docking

Diabetes

### ABSTRACT

QSAR modelling and docking studies on 45 thiazole analogues were carried out. The studied compounds in this research were optimized adopting DFT method at B3LYP function with a 6-31G\* basis set. The QSAR models were generated in material studio by MLR analysis (GFA method). Based on its statistical fitness, the first model was selected and reported as the best model and assessed with  $R^2 = 0.906134$ ,  $R^2 \text{ adj} = 0.89049$ ,  $Q^2 \text{ cv} = 0.86149$  and  $R^2 \text{ pred} = 0.82581$  statistical parameters. The ligand with the highest binding energy of -11.0 kcal/mol among the other ligands was ligand 13 as indicated by the molecular docking. The standard drug (acarbose) was also docked to the binding pocket of  $\alpha$ -glucosidase with -9.5kcal/mole docking score. The most active compound was found to be better than standard drug. The outcome of this findings paved way for predicting novel  $\alpha$ -glucosidase inhibitors having improved potency toward their target enzyme.

## 1. INTRODUCTION

The essential role played by  $\alpha$ -glucosidase in the breaking down of carbohydrate in the body makes it an important enzyme. It catalyzes the breaking down of carbohydrate, resulting in the discharge of too much sugar. It is situated inside the small bowel at the epithelium tissue of the small intestine (Wang *et al.*, 2016). Inhibitors of  $\alpha$ -glucosidase are kinds of small molecules (drugs) used in curing non-insulin dependent diabetes mellitus (NIDDM) by inhibiting  $\alpha$ -glucosidase (Taha *et al.*, 2015). Inhibitors of  $\alpha$ -glucosidase are used in the treatment of NIDDM (Kavitha *et al.*, 2017). Inhibitors of  $\alpha$ -glucosidase can also stop some other diseases like hepatitis, cancer, and HIV (Li *et al.*, 2004).

Thiazole is a five-membered azole heterocyclic organic compound containing a ring of 3 carbon atoms, a nitrogen and a sulphur (Taha *et al.*, 2016). Thiazole and its derivatives have wide industrial application in pharmacy, liquid crystals, and polymers (de Souza, 2005). Thiazoles have several biological activities such as antioxidant, insecticidal, antitumor, anticonvulsant, anti-hyperlipidemic and anti-inflammatory (Khan *et al.*, 2016)

Computer-aided drug design (CADD) is a unique area in drug discovery arena which apply the concept of molecular modelling to study the interaction between drugs and their

target protein (Bibi and Sakata, 2016). QSAR is a molecular modeling technique widely used to correlate physicochemical properties of compounds and their experimentally determined activities (Alisi *et al.*, 2018). While molecular docking is used to study the possible orientation of the target protein to the ligand when they bind to one another to form complex (Abdulfatai *et al.*, 2017). This research is aimed at performing computational modelling and docking on thiazole analogues against  $\alpha$ -Glucosidase receptor.

## 2. Materials and Method

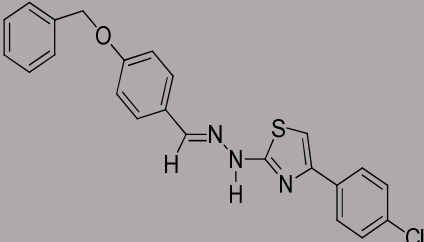
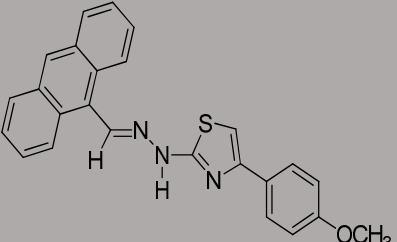
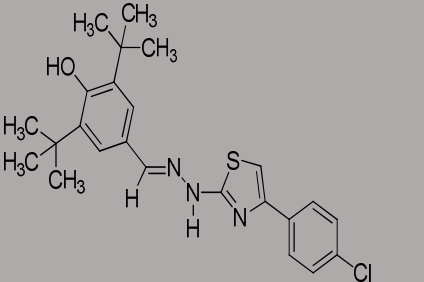
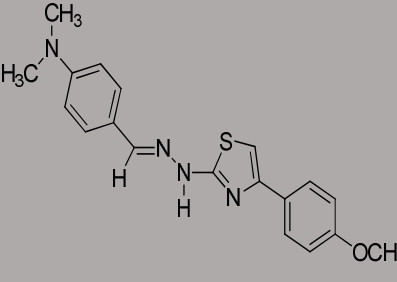
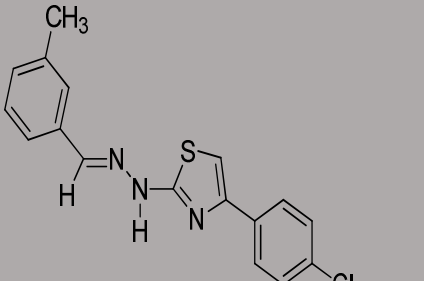
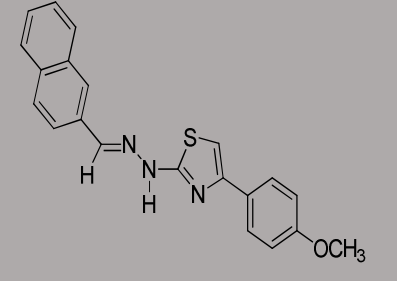
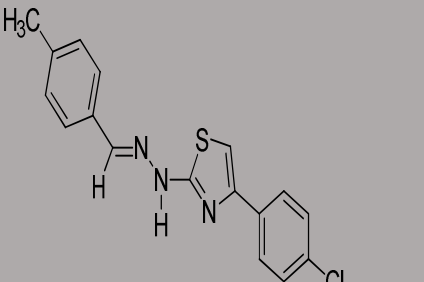
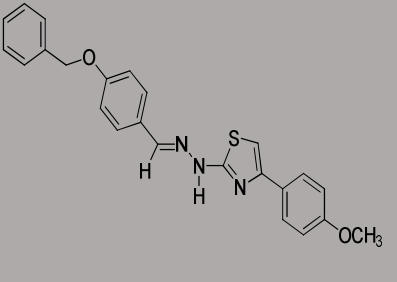
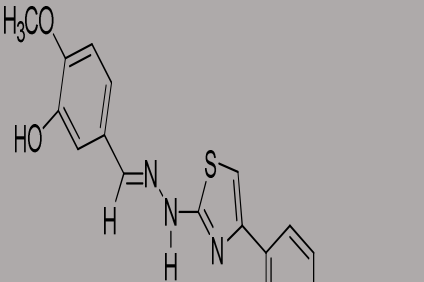
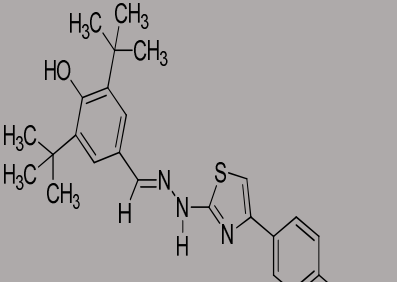
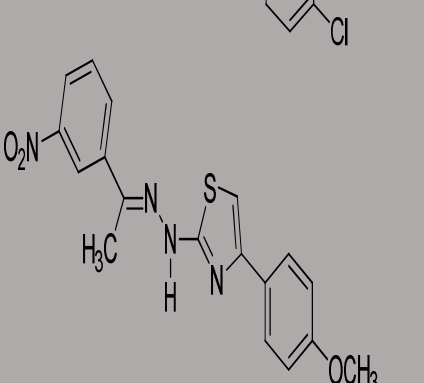
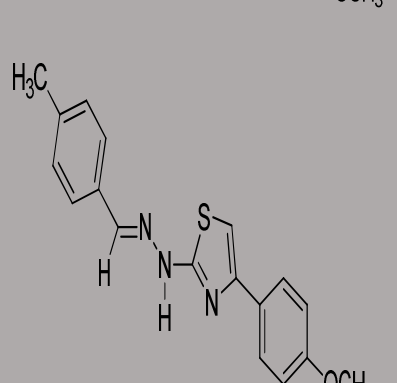
### 2.1 QSAR studies

#### 2.1.1 Sources of the Dataset

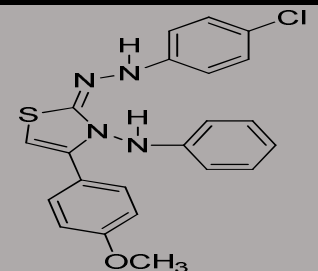
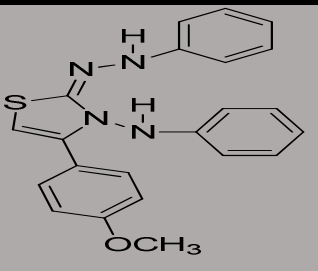
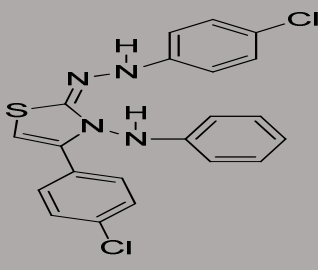


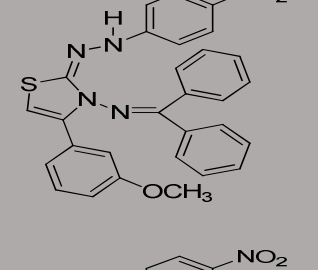
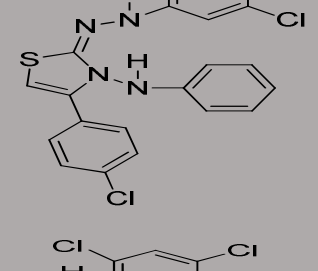

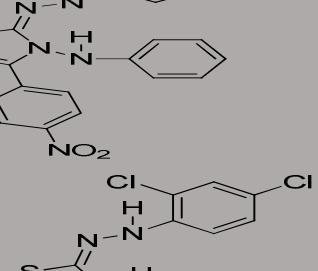
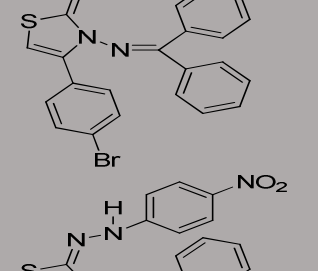
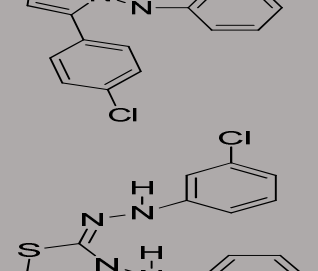
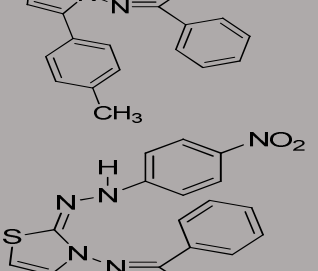
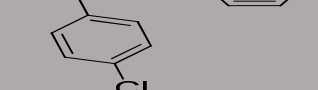
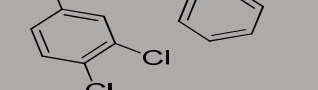
45 analogues of the studied compounds and their  $\alpha$ -glucosidase inhibitory activities ( $IC_{50}$ ) were downloaded from the work of (Rahim *et al.*, 2015) and (Khan *et al.*, 2016) for the purpose of this research. The inhibitory activities ( $IC_{50}$ ) ( $\mu$ M) of the dataset were converted to  $pIC_{50}$  (Ibrahim *et al.*, 2018a). 45 sets of the studied compounds and their inhibitory activities were presented in Table 1. ( $pIC_{50} = \log_1/IC_{50}$ ).

**Table 1-The normalized activity ( $pIC_{50}$ ) and the structures of the studied compounds**

S/No	Structures	$pIC_{50}$	S/No	Structures	$pIC_{50}$
1		2.34	4		2.59
2		1.64	5		2.31
3		2.38	6		2.24

S/No	Structures	pIC <sub>50</sub>	S/No	Structures	pIC <sub>50</sub>
7		1.57	13		2.28
8		1.26	14		2.16
9		1.84	15		2.29
10		2.53	16		2
11		2.25	17		2.09
12		2.63	19		2.35

S/No	Structures	pIC <sub>50</sub>	S/No	Structures	pIC <sub>50</sub>
20		2.24	26		1.92
21		1.67	27		1.54
22		1.37	28		1.42
23		1.36	29		1.15
24		1.35	30		1.25
25		1.42	31		1.43

S/No	Structures	pIC <sub>50</sub>	S/No	Structures	pIC <sub>50</sub>
32		1.28	39		1.51
33		0.98	40		1.69
34		1.11	41		1.7
35		1.08	42		1.86
36		1.23	43		1.86
37		1.1	44		1.67
38		1.21	45		1.69

## 2.1.2 Geometry optimization and Calculation of descriptors.

The 2D structures of these compounds were drawn using ChemDraw Ultra version 12.0. The studied compounds in this research were optimized utilizing B3LYP version of DFT method with 6-31G\* basis set (Abdulfatai *et al.*, 2017). PaDEL descriptor software was used to compute both thermodynamic, topological, autocorrelation constitutional, electronic, and geometric descriptors (Amin and Gayen, 2016) for further studies (Yap, 2011)

## 2.1.3 Dataset splitting and Correlation Analysis.

The dataset was randomly split into a model set (training set) of 36 molecules used to build the QSAR model and 9 validation set (test set) used for the validation of the built QSAR models (Cheng *et al.*, 2014).

GFA method was employed for the correlation analysis using the normalized activities (pIC<sub>50</sub>) as the response/dependent variable and the descriptors as independent variables (Arthur *et al.*, 2016).

## 2.1.4 Validation of the QSAR Model.

The generated QSAR models were judged using leave-one-out cross validation coefficient Q<sup>2</sup><sub>LOO</sub> parameter. R<sup>2</sup> is an important parameter for validation of a QSAR models and it is given below:

$$R^2 = 1 - \frac{\sum(Y_{exp} - Y_{prd})^2}{\sum(Y_{exp} - Y_{mtrng})^2} \quad 1$$

where Y<sub>exp</sub> is the experimental activity, Y<sub>pred</sub> is the predicted activity, and Y<sub>mtraining</sub> is the mean of the experimental activity of the model set (Adeniji *et al.*, 2018).

The R<sup>2</sup><sub>test</sub> value of the generated model is also very paramount need to be calculated and is defined as:

$$R^2_{test} = 1 - \frac{\sum(Y_{prd} - Y_{exp})^2}{\sum(Y_{exp} - Y_{mtrng})^2} \quad 2$$

where Y<sub>exp</sub> is the experimental activity, Y<sub>pred</sub> is the predicted activity, and Y<sub>mtraining</sub> is the mean of the experimental activity of the validation set (Tropsha *et al.*, 2003).

## 2.1.5 Applicability domain

Applicability domain is carried out to investigate the compounds with cross-validated standardized residuals greater than 3δ (outliers) and compounds with leverages greater than the warning leverage (influential compounds)(Tropsha *et al.*, 2003). In this regard, Leverage approach is used and is represented as h<sub>i</sub>:

$$h_i = x_i (X^T X)^{-1} x_i^T \quad (i=K, \dots, P) \quad 3$$

The threshold (h\*) is given as:

$$h^* = 3(p+1)/N \quad 4$$

where p represent the number of descriptors in the model and N is the number of compounds in the model set.

## 2.1.6 MLR Y-randomization Test.

MLR Y-randomization test (<sup>c</sup>R<sub>p</sub><sup>2</sup>) of the best model was carried out to ensure that the model was not gotten by chance. The strength of the best model was confirmed by the high low R<sup>2</sup> and Q<sup>2</sup> values for many trials (Adedirin *et al.*, 2018). <sup>c</sup>R<sub>p</sub><sup>2</sup> is given by equation 5.

$${}^cR_p^2 = R^*(R^2 - (\text{average } R_r)^2)^{1/2} \quad (5)$$

## 2.2.0 Docking analysis.

The interaction between the receptor (α-glucosidase) and the ligands (Thiazole analogues) was studied using molecular docking. The ligands were prepared by saving the structures of the studied compounds in pdb file format for this analysis (Abdulfatai *et al.*, 2017). The crystal structure of the target enzyme (α-glucosidase) with this ID 3AJ7 was downloaded from Protein Databank (PDB). The receptor was prepared with the aid of Discovery studio software (Veeramany *et al.*, 2011) and save as PDB. The prepared structures of the ligand and the receptor were shown in Figures 1 and 2. Autodock vina of pyrex software was used to dock the ligands (Thiazole analogues) to the binding pocket of the target enzyme (α-glucosidase) (Trott and Olson, 2010). One of the limitations of docking with Auto-dock vina of Pyrex is that the ligand and the receptor separated (decoupled) after carrying out the docking. Therefore, chimera was utilized for the recoupling of the ligands and the α-glucosidase (rebuilding the complexes).Discovery studio visualizer was used for the visualization of the complexes to study their nature of interactions.

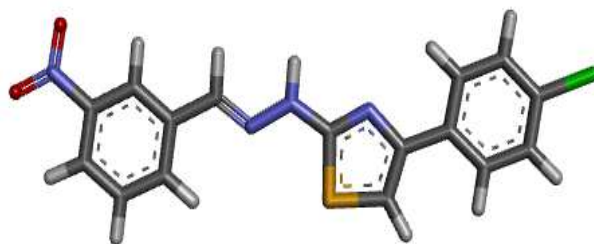


Figure 1 - 3D structure of the prepared Ligand.

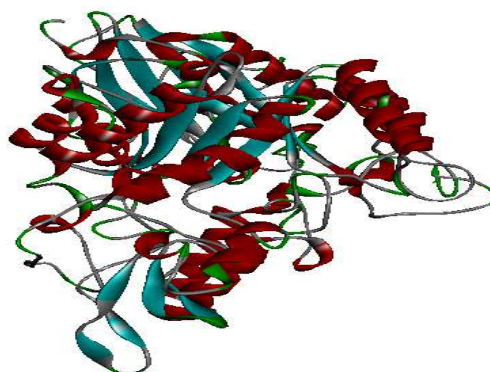


Figure 2 - 3D structure of the prepared Receptor.

### 3. Result and Discussion.

#### 3.1 QSAR Results of the studied compounds

The MLR analysis was done employing GFA method to develop the models. The first model was selected as the studied model based on its statistical fitness as it has LOF value of 0.101072,  $R^2$  value of 0.906134,  $R^2_{adj}$  value of 0.89049,  $Q^2_{LOO}$  value of 0.86149 and the  $R^2_{pred}$  value of 0.825811. The minimum accepted values for a suitable QSAR model validation is given in Table 2 (Ibrahim *et al.*, 2018b).

**Table 2- The minimum accepted values for a suitable QSAR model validation**

Symbol	Name	Value
$R^2$	Co-efficient of determination	$\geq 0.6$
$P_{(95\%)}$	Confidence interval at 95% confidence level	$< 0.05$
$Q^2$	Cross-validation co-efficient	$\geq 0.5$
$R^2 - Q^2$	Difference between $R^2$ and $Q^2$	$\leq 0.3$
$N_{(ext. \& test set)}$	Minimum number of external and test set	$\geq 05$
$R^2_{ext.}$	Co-efficient of determination of external and test set	$\geq 0.5$

#### Model 1

$$pIC_{50} = - 5.991927534 * AATSC8p + 9.285263403 * SpMin7_Bhv + 2.306067733 * SpMax7_Bhe - 8.385632034 * SpMin7_Bhp - 5.904841760 * SpMax3_Bhi + 16.07991271.$$

$$R^2 = 0.906134 \quad R^2_{adj} = 0.89049, \quad Q^2_{LOO} = 0.86149, \quad N_{trng} = 36,$$

$$R^2_{test} = 0.825811, \quad N_{test} = 9, \quad LOF = 0.101072.$$

The negative coefficient of these independent variables **AATSC8p**, **SpMax3\_Bhi**, and **SpMin7\_Bhp** in the model suggest that when the values of these independent variables in the thiazoles analogues are decreased, the inhibitory activity of these anti-diabetic compounds against  $\alpha$ -glucosidase will be improved, Whereas increasing such independent variables will reduce the inhibitory activity of these compounds against  $\alpha$ -glucosidase, meaning that these independent variables contributed negatively to the inhibitory activity of these compounds. Also, the positive coefficient of **SpMin7\_Bhv** and **SpMax7\_Bhe** independent variables suggest that adding such independent variables will improve the activity of these anti-diabetic compounds against  $\alpha$ -glucosidase. The higher the value of this independent variables, the better the anti-diabetic activity of these compounds against  $\alpha$ -glucosidase. This implies that these independent variables contributed positively to the inhibitory activity of the thiazoles analogues. The names, definitions, and category of the descriptors in the selected model were presented in Table 3.

The graph of predicted activities of both the model building sets and validation sets versus the inhibitory activities ( $pIC_{50}$ ) is presented in Figure 3. It can be seen from the graph that the internal validation  $R^2$  value of the training set agrees with the  $R^2$  value of 0.8061 extrapolated from the graph which affirmed the strength, reliability and robustness of the selected model.

In order to confirm the absence of systematic error in the selected model, Actual activities was plotted against standardized residuals. The even distribution of these residuals in Figure 4 on either side of zero indicates that the selected model was free from systematic error.

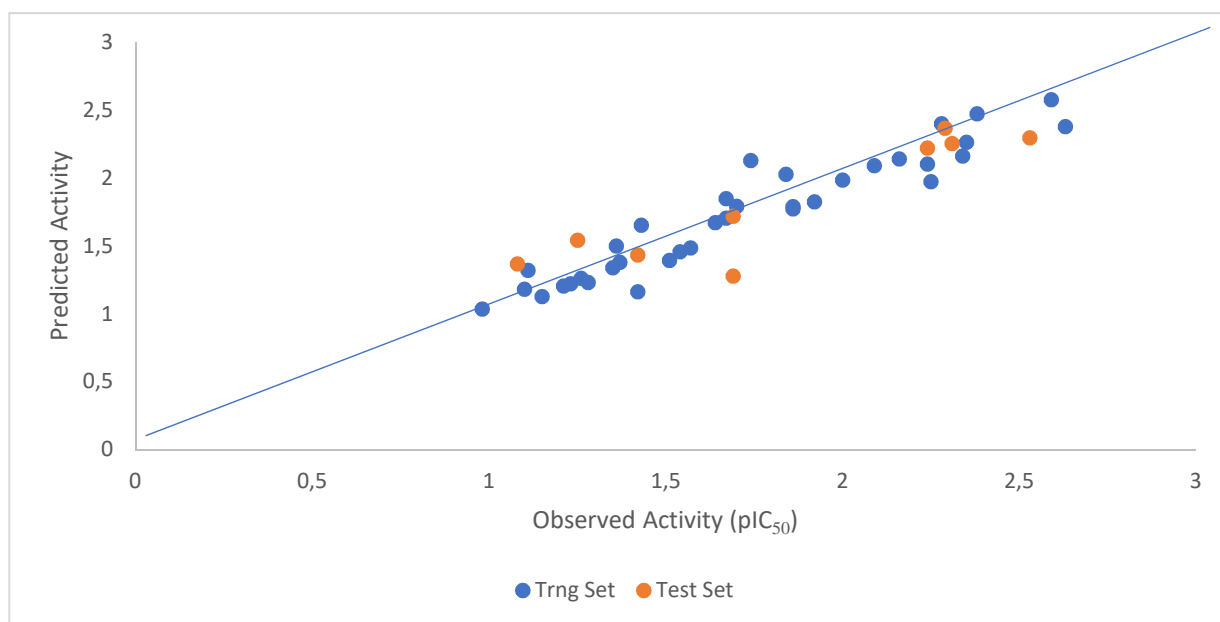
The high predictive ability of the selected model was confirmed by the low residual values observed between the Actual activities ( $pIC_{50}$ ) and the Predicted activities ( $pIC_{50}$ ) in Table 4.

**Table 3-The names, definitions, and category of the descriptors that appear in the selected model**

S/No	Name	Definition	Category
1	<b>AATSC8p</b>	Average centered Broto-Moreau autocorrelation - lag 8 / weighted by polarizabilities.	2D
2	<b>SpMin7_Bhv</b>	The largest absolute eigenvalue of Burden modified matrix - n 7 / weighted by relative van der Waals volumes.	2D
3	<b>SpMax7_Bhe</b>	The largest absolute eigenvalue of Burden modified matrix - n 7 / weighted by relative Sanderson electronegativities.	2D
4	<b>SpMin7_Bhp</b>	The smallest absolute eigenvalue of Burden modified matrix - n 7 / weighted by relative polarizabilities	2D
5	<b>SpMax3_Bhi</b>	The largest absolute eigenvalue of Burden modified matrix - n 3 / weighted by relative first ionization potential	2D

**Table 4-The  $pIC_{50}$ , Predicted ( $pIC_{50}$ ) and Residual of the selected Model**

S/No.	$pIC_{50}$	Predicted $pIC_{50}$	Residual	S/No.	$pIC_{50}$	Predicted $pIC_{50}$	Residual
M001	2.34	2.163252	0.176748	M0024	1.35	1.340045	0.009955
M002	1.64	1.671857	-0.03186	M0026	1.92	1.82598	0.09402
M003	2.38	2.473876	-0.09388	M0027	1.54	1.45742	0.08258
M004	2.59	2.577783	0.012217	M0028	1.42	1.163053	0.256947
M006	2.24	2.10412	0.13588	M0029	1.15	1.127712	0.022288
M007	1.57	1.485451	0.084549	M0031	1.43	1.653718	-0.22372
M008	1.26	1.261678	-0.00168	M0032	1.28	1.230159	0.049841
M009	1.84	2.028562	-0.18856	M0033	0.98	1.03571	-0.05571
M0011	2.25	1.973986	0.276014	M0034	1.11	1.320836	-0.21084
M0012	2.63	2.379583	0.250417	M0036	1.23	1.222137	0.007863
M0013	2.28	2.400443	-0.12044	M0037	1.1	1.181313	-0.08131
M0014	2.16	2.141774	0.018226	M0038	1.21	1.204513	0.005487
M0016	2	1.986361	0.013639	M0039	1.51	1.393759	0.116241
M0017	2.09	2.092718	-0.00272	M0041	1.7	1.791219	-0.09122
M0018	1.74	2.129947	-0.38995	M0042	1.86	1.774504	0.085496
M0019	2.35	2.262639	0.087361	M0043	1.86	1.790044	0.069956
M0021	1.67	1.849764	-0.17976	M0044	1.67	1.704178	-0.03418
M0022	1.37	1.379203	-0.0092				
M0023	1.36	1.500701	-0.1407				



**Figure 3-The plot of  $pIC_{50}$  and Predicted  $pIC_{50}$  of both the model and validation sets of the selected model.**

The predicted activities and residuals of the test set for the selected model were calculated and shown in Table 5 which further confirmed the high predictive ability of the

selected model. The Computation of predictive  $R^2$  shown in Table 6 further confirmed the robustness and reliability of the selected model.



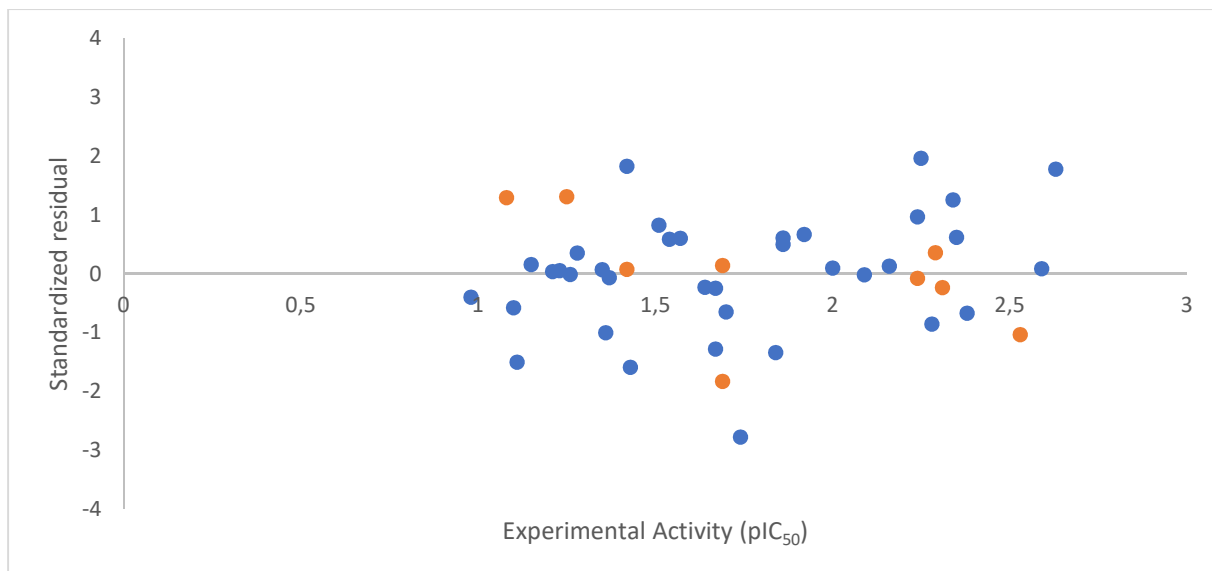


Figure 4-The plot of the Residual and pIC<sub>50</sub> of the selected model.

Table 5-Computation of pIC<sub>50</sub> (predicted) and residuals of the validation set of the selected model

pIC <sub>50</sub>	AATSC8p	SpMin7_Bhv	SpMax7_Bhe	SpMin7_Bhp	SpMax3_Bhi	Y <sub>prd</sub>	Y <sub>prd</sub> -Y <sub>obs</sub>
2.31	0.02102	1.12975	2.77182	1.05826	3.67607	2.25508	-0.0549
2.53	-0.035	1.00717	2.77182	0.96028	3.67238	2.29632	-0.2337
2.29	0.01892	1.17481	2.95111	1.1323	3.69485	2.36787	0.07787
2.24	0.01171	1.13687	2.86851	1.10062	3.68024	2.22016	-0.0198
1.42	0.01627	1.24737	3.00503	1.21827	3.86868	1.43454	0.01454
1.25	-0.0102	1.25682	2.94436	1.23031	3.85148	1.54138	0.29138
1.08	-0.0151	1.00717	2.87537	0.96028	3.84982	1.36791	0.28791
1.69	-0.0292	1.33475	3.26554	1.40219	3.91931	1.27785	-0.4121
1.69	-0.0251	1.2809	3.13963	1.26558	3.90035	1.72007	0.03007

Table 6-Computation of predictive R<sup>2</sup> of the selected model

S/No.	(Y <sub>prd</sub> -Y <sub>obs</sub> ) <sup>2</sup>	Ȳ <sub>trng</sub>	Y <sub>obs</sub> -Ȳ <sub>trng</sub>	(Y <sub>obs</sub> -Ȳ <sub>trng</sub> ) <sup>2</sup>
5	0.00302	1.7244	0.5856	0.34293
10	0.05461	1.7244	0.8056	0.64899
15	0.00606	1.7244	0.5656	0.3199
20	0.00039	1.7244	0.5156	0.26584
25	0.00021	1.7244	-0.3044	0.09266
30	0.0849	1.7244	-0.4744	0.22506
35	0.08289	1.7244	-0.6444	0.41525
40	0.16987	1.7244	-0.0344	0.00118
45	0.0009	1.7244	-0.0344	0.00118
Σ(Y <sub>prd</sub> -Y <sub>obs</sub> ) <sup>2</sup> =0.4029				Σ(Y <sub>obs</sub> -Ȳ <sub>trng</sub> ) <sup>2</sup> =2.313
R <sup>2</sup> = 1 - (0.4029/2.313) = 0.8258				

The Pearson's correlation was carried out on the independent variable that appear in the selected model (Table 7). This indicates that the independent variable utilized in generating the model were of good quality. Also,

the importance and contribution of the independent variable that appear in the selected model were determine using their mean effect values (Table 7).

**Table 7-Pearson's correlation analysis of the descriptors in the studied model**

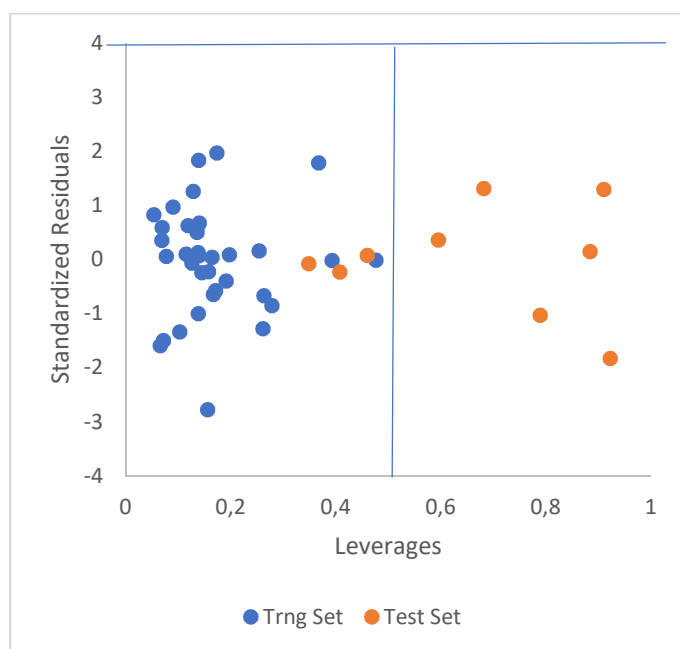
	AATSC8p	SpMin7_Bhv	SpMax7_Bhe	SpMin7_Bhp	SpMax3_Bhi	MF
AATSC8p	1					0.001173
SpMin7_Bhv	0.001986	1				-0.74996
SpMax7_Bhe	-0.3452	0.837262	1			-0.47028
SpMin7_Bhp	-0.13042	0.981499	0.904859	1		0.658535
SpMax3_Bhi	-0.45466	0.448907	0.64831	0.516989	1	0.679415

The applicability domain was shown by plotting the Williams plot (standardized residuals against leverages) as shown in Figure 5. It can be seen from the plot that 6 compounds in the test set have their leverages value greater than the threshold value  $h^*(h^*=0.5)$ . These compounds are called influential compounds and they are not considered when designing new other ones with improved activities

because the model cannot predict their activities. The MLR Y-randomization test is carried to assess the robustness of the selected model. It is shown in Table 8 that the selected model was robust and was not obtained by chance because the new parameter ( $cRp^2$ ) obtained was greater than 0.5 (0.606241).

**Table 8-MLR Y-randomization result**

Model	R	R <sup>2</sup>	Q <sup>2</sup>
Original	0.817486	0.668283	0.543764
Random 1	0.435427	0.189597	-0.07775
Random 2	0.596614	0.355949	0.145902
Random 3	0.581513	0.338158	0.11225
Random 4	0.231249	0.053476	-0.24571
Random 5	0.227931	0.051953	-0.26512
Random 6	0.320037	0.102423	-0.16722
Random 7	0.382972	0.146668	-0.14174
Random 8	0.317907	0.101065	-0.21706
Random 9	0.282764	0.079956	-0.25776
Random 10	0.063417	0.004022	-0.34226
Random Models Parameters			
Average r :	0.343983		
Average r <sup>2</sup>		0.142327	
:			
Average Q <sup>2</sup> :	-0.14565		
cRp <sup>2</sup> :	0.606241		



**Figure 5-Williams plot.**

## Docking studies Results

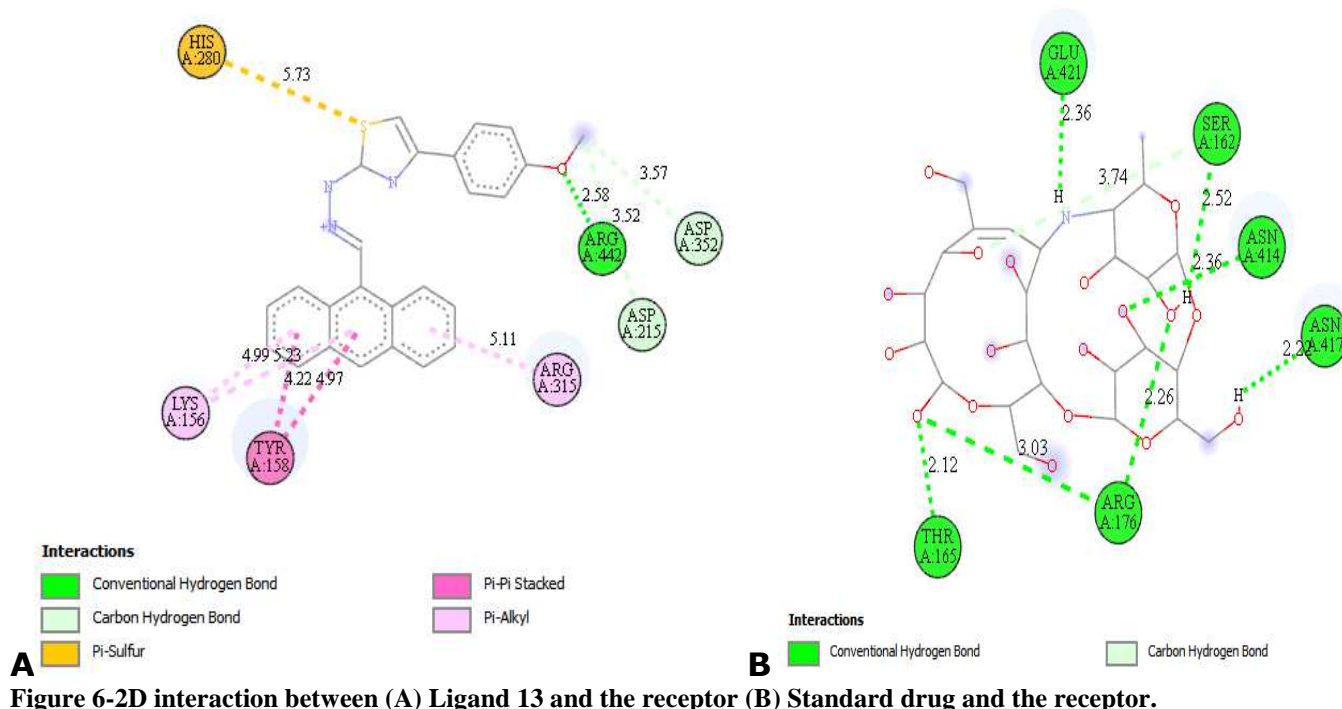
45 sets of thiazole analogues (Ligands) were docked against  $\alpha$ -glucosidase (receptor). The results of the docking analysis in Table 9 clearly showed that ligand number 13 has the highest binding energy of -11.0kcal/mole and formed hydrogen bond interactions with ARG442 (2.5752A°), hydrophobic interactions with active residues such as TYR158, LYS156, ARG315, LYS156, electrostatic interaction with HIS280 and carbon-hydrogen bond with

ASP215 (3.5158 A°), ASP352 (3.5652 A°). The standard drug (acarbose) was also docked to the binding pocket of  $\alpha$ -glucosidase with -9.5kcal/mole docking score. It formed 8 hydrogen bond interactions with GLU421 (2.36494A°), ASN417 (2.22115A°), SER162 (2.51822A°), THR165 (2.12267A°), ARG176 (3.03496A°), ARG176 (2.25819A°), ASN414 (2.36034A°) and SER162 (3.7388A°) of  $\alpha$ -glucosidase. Figure 6A and B showed the 2D interaction between ligand 13- receptor and Standard drug - receptor.

**Table 9-Summary of the interactions between  $\alpha$ -glucosidase and the ligands**

Ligands-Receptor	Binding Energy(kcal/mol)	Hydrophobic Interaction	Electrostatic Interaction/Others	Hydrogen Bonds	Hydrogen Bond Distance (Å)
1	-8.5	SER311, ARG315 and PRO312	ASP307	ASP307 and ARG442	2.8858 and 2.3897
2	-8.7	PHE303, TYR158, VAL216, TYR72, PHE178, and HIS280	GLU27 and ASP35	SER24 and SER240	2.0339 and 3.0898
3	-8.5	TRP15, ILE262, ARG263 and ILE272	GLU271	ILE272	3.0922
4	-9.7	ASP307, VAL308, PRO312, ARG315 and PHE303	ASP307	SER311, ASP307 and THR310	2.1107, 2.7360 and 2.0534
5	-8.2	TYR158, ASP307, VAL308, PRO312 and ARG315	ASP307	ASP307, THR310 and SER311	2.6514, 1.9988 and 2.8322
6	-9.3	ARG315, VAL308 and ALA329	ASP307	THR310 and ASP307	2.7397 and 2.2357
7	-9.1	VAL308, TYR158, ARG315, PRO312 and PHE178	ASP307	HIS280 and GLY309	2.9597 and 2.9829
8	-9.3	VAL216, ARG315, TYR72, HIS112, TYR158, PHE178 and PHE314	GLU411 and ASP352	GLU411	2.9724
9	-9.4	TYR158, PHE314, PHE314, LYS156 and ALA418	LYS156 and TRP238	ASN415, GLY161, SER157 and PHE314	2.2854, 2.6837, 3.7595 and 2.5113
10	-9.1	VAL216, ARG315, LYS156, TYR158, and PHE178	GLU411, ASP352, and PHE314		
11	-9.1	PHE314, LYS156, ALA418 and ILE419	LYS156 and TRP238	ASN415, GLY161, SER157 and PHE314	2.5364, 2.6937, 3.6267 and 2.5569
12	-9.4	PHE303, TYR158 and LYS156	HIS280	ASP242, ARG442, ASP215 and ASP352	2.6233, 2.6399, 3.5288 and 3.4713
13	-11.0	TYR158, LYS156, ARG315 and LYS156	HIS280	ARG442, ASP215 and ASP352	2.5752, 3.5158 and 3.5652
14	-8.2	TYR158, ASP307, VAL308, PRO312, ARG315 and PRO312	ASP307	ASP307, THR310, SER311 and ASP325	2.5887, 2.0332, 2.4954 and 3.6392
15	-9.8	TYR158, PHE178, ARG315, LYS156 And VAL216	GLU411, ASP352, PHE314 and TYR316	GLU411, ASP242 and TYR158	2.6801, 2.9945 and 3.6015
16	-9.4	TYR158, ASP307, VAL308, PRO312 and ARG315	ASP307 and ASP352	THR310, SER311, ASP307 and THR310	2.607, 2.1655, 2.5259 and 2.0355
17	-8.8	ARG315, PRO312 and PHE303	ASP307	THR310, SER311, ASP307, THR310 and SER311	2.3695, 2.3610, 2.6801, 2.0895 and 3.0555
18	-8.9	LYS156 and TYR158	ASP242, HIS280 and PHE303	HIS280, ARG442 and ASP215	2.6759, 2.4835 and 3.6948
19	-9.0	ALA292, TRP15, LEU297, SER298, VAL266, ARG263, ILE272 and LYS13		ILE272, ASN259, and GLU11	1.9759, 3.6456 and 3.4362
20	-8.8	ALA292, TRP15, SER291, ILE262 and ARG263	THR274	ASN259, GLU296, THR290, SER298, THR274, ARG263 and LEU297	2.7351, 2.3154, 1.9711, 2.9548, 2.3927, 3.4650 and 3.5142
21	-9.2	TYR158, ARG315 and LYS156	GLU411, ARG442, ASP352, PHE314 and TYR316	GLU277 and ASP352	2.1094 and 2.3821
22	-9.4	TYR158	ASP307 and ASP242	ASP307, and ARG442	3.0021 and 3.6732
23	-9.6	TYR158	ASP307 and ASP242	ASP307 and ARG442	3.0815 and 3.4567
24	-9.3	TYR158	ASP307 & ASP242	ASP307 and ARG442	3.0287 and 2.2548

Ligands-Receptor	Binding Energy(kcal/mol)	Hydrophobic Interaction	Electrostatic Interaction/Others	Hydrogen Bonds	Hydrogen Bond Distance (Å)
25	-8.4	HIS280, TYR158 and PRO312	ASP242 and ASP307	ASP242	2.1545
26	-9.3	TYR158 and PHE159	ASP307 and ASP242	ASP307	3.0050
27	-8.7	PHE321, LEU323, LEU318, LEU439, TRP326 and PHE360		THR358 and GLY361	2.4937 and 2.1589
28	-9.0	TYR158 and PHE178	ASP242	PRO312, LYS156 and SER240	2.0603, 2.1594 and 2.0578
29	-8.9	ARG315 and PRO312	ASP242 and ASP307	GLY160 and ASN415	2.989 and 2.1150
30	-8.9	TYR158, LYS156 and ARG315	GLU411, ASP307 and TYR158	SER241 and ASP242	1.8706 and 2.5307
31	-9.1	ARG315 and TYR158	ASP242	PRO312, LYS156 and SER240	1.9013, 1.9331 and 1.7843
32	-8.8	SER240 and TYR158	ASP242	PRO312	1.8459
33	-9.1	ARG315, TYR158 and PHE159	ASP242	PRO312	1.8991
34	-9.8	PRO312, TYR158, HIS280, PRO312, ARG315 and HIS280	ASP307	ASP307, SER311, SER241, SER240 and ARG315	2.9473, 2.7324, 1.8218, 3.0827 and 2.9212
35	-9.1	HIS280, VAL232, ARG315 and TYR158	ASP242	PRO312	2.7322
36	-9.9	PRO312, TYR158, PRO312, ARG315 and HIS280	ASP307	SER311, SER241, SER240 and ARG315	2.8039, 1.8313, 3.0822 and 2.9219
37	-8.9	HIS280, VAL232, LEU313, TYR158 and PHE159	ASP242		
38	-9.1	PHE303, LYS156, TYR158 and PHE178	ASP307		
39	-8.4	ARG263, VAL266, and ALA292		ASN259, THR290, and SER298	2.4738, 3.3492 and 2.7081
40	-8.3	PHE321	TRP581	GLY361, LEU323 and LYS523	2.3735, 2.1644 and 2.3789
41	-8.1	PHE321, LEU323, and LYS523		ASP363	1.9111
42	-7.7	ALA418 and LYS148	GLU421, ARG176, and PHE173	TRP164, ASN414, and ARG176	2.6508, 2.7899 and 3.4268
43	-9.0	HIS280, TYR158, PHE303, VAL232, LEU313, PRO312, ARG315	ASP242, ASP307 and TYR158	HIS280, ARG315 and ARG315	2.5372, 2.6795 and 2.5501
44	-7.7	ALA418 and LYS148	GLU421, ARG176, and PHE173	TRP164, ASN414, and ARG176	2.6530, 2.7260 and 3.4199
45	-9.0	TYR158, VAL216, ARG315, PHE159, PHE178, and PHE303	ASP307, ASP242, and HIS280		
<b>Std drg-Receptor</b>	<b>-9.</b>			<b>GLU421, ASN417, SER162, THR165, ARG176, ARG176, ASN414 and SER162</b>	<b>2.36494, 2.22115, 2.51822, 2.12267, 3.03496, 2.25819, 2.36034 and 3.7388</b>



#### 4. Conclusion.

Computational Studies on 45 studied compounds as  $\alpha$ -glucosidase inhibitors were carried out. Based on the assessment carried out, the first model was selected as the studied model and assessed with LOF value of 0.101072,  $R^2$  value of 0.906134,  $R^2_{adj}$  value of 0.89049,  $Q^2_{LOO}$  value of 0.86149 and the  $R^2_{pred}$  value of 0.825811. The QSAR result of this study indicates the effects of the descriptors **AATSC8p**, **SpMax3\_Bhi**, and **SpMin7\_Bhp** as they contributed negatively to the inhibitory activities of the thiazole analogues. While **SpMin7\_Bhv** and **SpMax7\_Bhe** have positive effects toward the inhibitory activities of the compounds. The docking study clearly showed that ligand number 13 has the highest binding energy (-11.0) kcal/mole and formed hydrogen bonding with ARG442 ( $2.5752\text{\AA}$ ), hydrophobic interaction with active residues such as TYR158, LYS156, ARG315, LYS156, electrostatic interaction with HIS280 and carbon-hydrogen bond with ASP215 ( $3.5158\text{\AA}$ ), ASP352 ( $3.5652\text{\AA}$ ). The standard drug (acarbose) was also docked to the binding pocket of  $\alpha$ -glucosidase with -9.5kcal/mole docking score. The most active compound was found to be better than standard drug acarbose. We hope this research may give the basis for the designing of new thiazole derivatives with better inhibitory activities.

#### Acknowledgments

The authors sincerely acknowledge Ahmadu Bello University, Zaria for its technical support and Abdulfatai Usman for his advice in the course of this research.

#### REFERENCES

- Abdulfatai, U., Uzairu, A., and Uba, S. (2017). Quantitative structure-activity relationship and molecular docking studies of a series of quinazolinonyl analogues as inhibitors of gamma amino butyric acid aminotransferase. *Journal of advanced research*, 8(1), 33-43.
- Adedirin, O., Uzairu, A., Shallangwa, G. A., and Abechi, S. E. (2018). QSAR and molecular docking based design of some n-benzylacetamide as  $\gamma$ -aminobutyrate-aminotransferase inhibitors. *The Journal of Engineering and Exact Sciences*, 4(1), 0065-0084.
- Adeniji, S. E., Uba, S., and Uzairu, A. (2018). Quantitative structure-activity relationship and molecular docking of 4-Alkoxy-Cinnamic analogues as anti-mycobacterium tuberculosis. *Journal of King Saud University-Science*.
- Alisi, I. O., Uzairu, A., Abechi, S. E., and Idris, S. O. (2018). Quantitative Structure Activity Relationship Analysis of Coumarins as Free Radical Scavengers by Genetic Function Algorithm. *Physical Chemistry Research*, 6(1), 209-223.
- Amin, S. A., and Gayen, S. (2016). Modelling the cytotoxic activity of pyrazolo-triazole hybrids using descriptors calculated from the open source tool

- "PaDEL-descriptor". *Journal of Taibah University for Science*, 10(6), 896-905.
- Arthur, D. E., Uzairu, A., Mamza, P., Abechi, S. E., and Shallangwa, G. (2016). Insilco study on the toxicity of anti-cancer compounds tested against MOLT-4 and p388 cell lines using GA-MLR technique. *Beni-Suef University Journal of Basic and Applied Sciences*, 5(4), 320-333.
- Bibi, S., and Sakata, K. (2016). Current status of computer-aided drug design for type 2 diabetes. *Current computer-aided drug design*, 12(2), 167-177.
- Cheng, L. P., Huang, X. Y., Wang, Z., Kai, Z. P., and Wu, F. H. (2014). Combined 3D-QSAR, molecular docking, and molecular dynamics study on potent cyclohexene-based influenza neuraminidase inhibitors. *Monatshefte für Chemie-Chemical Monthly*, 145(7), 1213-1225.
- de Souza, M. V. N. (2005). Synthesis and biological activity of natural thiazoles: An important class of heterocyclic compounds. *Journal of Sulfur Chemistry*, 26(4-5), 429-449.
- Ibrahim, M. T., Uzairu, A., Shallangwa, G. A., and Ibrahim, A. (2018a). Computational studies of some biscoumarin and biscoumarin thiourea derivatives as  $\alpha$ -glucosidase inhibitors. *The Journal of Engineering and Exact Sciences*, 4(2), 0276-0285.
- Ibrahim, M. T., Uzairu, A., Shallangwa, G. A., and Ibrahim, A. (2018b). In-silico studies of some oxadiazoles derivatives as anti-diabetic compounds. *Journal of King Saud University-Science*.
- Kavitha, S., Kannan, K., and Gnanavel, S. (2017). Synthesis, characterization and biological evaluation of novel 2, 5 substituted-1, 3, 4 oxadiazole derivatives. *Saudi Pharmaceutical Journal*, 25(3), 337-345.
- Khan, K. M., Qurban, S., Salar, U., Taha, M., Hussain, S., Perveen, S., Hameed, A., Ismail, N. H., Riaz, M., and Wadood, A. (2016). Synthesis, in vitro  $\alpha$ -glucosidase inhibitory activity and molecular docking studies of new thiazole derivatives. *Bioorganic chemistry*, 68, 245-258.
- Li, W., Zheng, H., Bukuru, J., and De Kimpe, N. (2004). Natural medicines used in the traditional Chinese medical system for therapy of diabetes mellitus. *Journal of ethnopharmacology*, 92(1), 1-21.
- Rahim, F., Ullah, H., Javid, M. T., Wadood, A., Taha, M., Ashraf, M., Shaikat, A., Junaid, M., Hussain, S., and Rehman, W. (2015). Synthesis, in vitro evaluation and molecular docking studies of thiazole derivatives as new inhibitors of  $\alpha$ -glucosidase. *Bioorganic chemistry*, 62, 15-21.
- Taha, M., Ismail, N. H., Imran, S., Selvaraj, M., and Rahim, F. (2016). Synthesis of novel inhibitors of  $\beta$ -glucuronidase based on the benzothiazole skeleton and their molecular docking studies. *RSC Advances*, 6(4), 3003-3012.
- Taha, M., Ismail, N. H., Lalani, S., Fatmi, M. Q., Siddiqui, S., Khan, K. M., Imran, S., and Choudhary, M. I. (2015). Synthesis of novel inhibitors of  $\alpha$ -glucosidase based on the benzothiazole skeleton containing benzohydrazide moiety and their molecular docking studies. *European journal of medicinal chemistry*, 92, 387-400.
- Tropsha, A., Gramatica, P., and Gombar, V. K. (2003). The importance of being earnest: validation is the absolute essential for successful application and interpretation of QSPR models. *Molecular Informatics*, 22(1), 69-77.
- Trott, O., and Olson, A. J. (2010). AutoDock Vina: improving the speed and accuracy of docking with a new scoring function, efficient optimization, and multithreading. *Journal of computational chemistry*, 31(2), 455-461.
- Veerasingh, R., Rajak, H., Jain, A., Sivadasan, S., Varghese, C. P., and Agrawal, R. K. (2011). Validation of QSAR models-strategies and importance. *International Journal of Drug Design & Discovery*, 3, 511-519.
- Wang, G., Peng, Z., Wang, J., Li, J., and Li, X. (2016). Synthesis and biological evaluation of novel 2, 4, 5-triarylimidazole-1, 2, 3-triazole derivatives via click chemistry as  $\alpha$ -glucosidase inhibitors. *Bioorganic & medicinal chemistry letters*, 26(23), 5719-5723.
- Yap, C. W. (2011). PaDEL-descriptor: An open source software to calculate molecular descriptors and fingerprints. *Journal of computational chemistry*, 32(7), 1466-1474.